Available online at www.sciencedirect.com
SCIENCE DIRECT®
International Journal of Fatigue 25 (2003) 1271–1277
International Journal of Fatigue
www.elsevier.com/locate/ijfatigue

Effect of ring indentation on fatigue crack growth in an aluminum plate

Won-Kyun Lim [a,*], Jeong-Hoon Song [a], Bhavani V. Sankar [b]

[a] Department of Mechanical Engineering, MyongJi University, Yongin, Kyonggi-do 449-728, South Korea
[b] Department of Mechanical and Aerospace Engineering, University of Florida, Gainesville, FL 32611, USA

Abstract

In the present investigation, a more efficient method for retardation of fatigue crack growth is examined. Residual stresses were created around the crack tip by indenting a cracked panel with rigid ring punches. The residual stresses near the crack tip were evaluated using fracture mechanics principles with the Bueckner weight function. It was observed that a state of compressive residual stress is introduced inside the indentation area. Fatigue testing of an aluminum specimen with single edge crack showed that the significant retardation effects were observed after the application of the ring indentation. It is also shown that the ring-indentation process increases the total fatigue life.

Keywords: Ring indentation; Residual stresses; Fatigue crack growth; Weight function

1. Introduction

Fatigue life enhancement based on the introduction of residual stress fields around cracks are important in improving the fatigue performance of aircraft structures. Among various techniques developed for fatigue life enhancement are the applications of overloads [1,2], drilling stop holes [3] and pressing steel ball [4,5] at crack tips. However, there are some limitations to the practical use of these methods. For the overload method, the magnitude of overloads generally is limited since it must be below the failure load of the structure. The method of drilling stop holes can result in reduction in structural strength. Finally, the procedure of ball indentation is difficult in practice as it requires finding the precise position of crack tips in sheet structures.

One way to compensate for this decrease in fatigue life is to create plastic deformations around regions of high stress by using an indentation process. A suitable state of compressive residual stresses can be achieved around a notch or hole using the process. Sehgal and Kobayashi [6] have examined the detailed deformation characteristics involved in the plastic indentation. By indenting a circular punch into steel specimens, they induced compressive strains along the workpiece surfaces. Lee and Kang [7] have carried out a fatigue crack growth study on aluminum alloy specimens indented by a ring punch around holes. This process produced a marked improvement in fatigue life. Lim et al. [8] have also induced residual stresses onto pre-machined holes using a ring-indentation process near the fastener hole combined with cold-expansion. They obtained the retardation of cracks emanating from a circular hole in aluminum specimens.

The present investigation is undertaken to examine a more efficient method for the retardation of crack growth, using ring punches indented around cracks in a sheet structure. Residual stresses near a crack tip are evaluated by fracture mechanics approach using the Bueckner weight function. By fatigue testing of aluminum specimen with single edge crack, the retardation effects are measured after the application of the method. Our goal here is to show that the indentation process is very beneficial for obtaining an increase in fatigue lives of materials with a crack.

2. Experimental procedures

The fatigue test specimens were of the single edge notch type and were 50 mm wide and 300 mm in length.

* Corresponding author. Tel.: +82-31-330-6422; fax: +82-31-321-4959.
E-mail address: limwk@mju.ac.kr (W.-K. Lim).

0142-1123/$ - see front matter © 2003 Elsevier Ltd. All rights reserved.
doi:10.1016/j.ijfatigue.2003.08.011

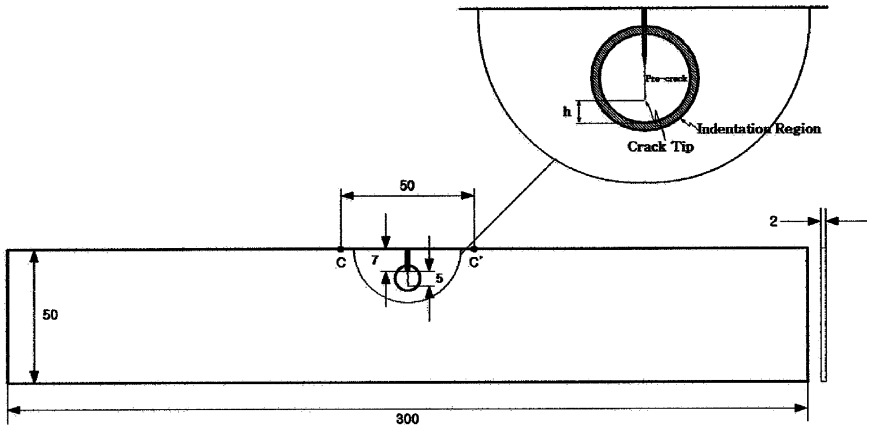

Fig. 1. Schematic of the A16061-T6 specimen (unit: mm).

Table 1
Mechanical properties of A1 6061-T6

Tensile strength (MPa)	318
Yield strength (MPa)	282
Elongation (%)	12
Modulus of elasticity (MPa)	68.9×10^3
Poisson's ratio	0.33

The geometrical details of the specimens are given in Fig. 1. The specimens were prepared from 2 mm thick 6061-T6 aluminum alloy. The specimens were cut from the plate such that the longitudinal axis of the specimen was aligned with the rolling direction. The mechanical properties of the specimen are given in Table 1. In order to start fatigue cracks, a saw cut of length 7 mm in the direction transverse to the long axis of the plate specimen was introduced at one edge of the specimen using a saw of 0.3 mm thick. The test specimens were pre-cracked to the length of 5 mm by applying zero-to-tension cyclic loads. After the pre-cracking process, the specimens were placed on a surface plate and the process of plastic indentation was preformed around cracks by using ring punches with an average diameter of 12.7 mm. Three types of ring punch, with different thickness of 0.5, 0.7 and 1.0 mm, were used as illustrated in Fig. 2. The ring punches had flat ends and were heat-treated.

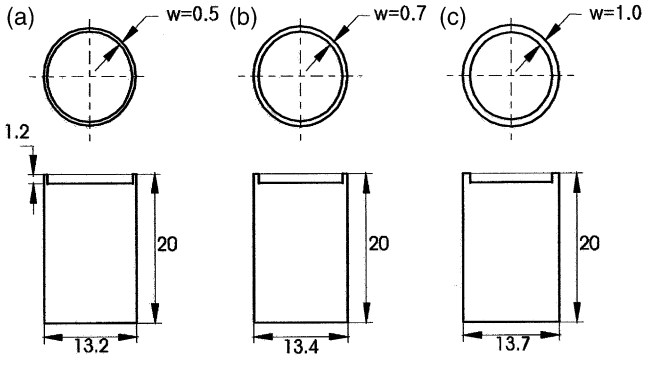

Fig. 2. Three types of ring punch used for indentation (unit: mm).

The indentations were located around cracks. The distances from the crack tip to the inner boundary of the ring ranged from 1 to 5 mm. Three different indentation depths, 0.06, 0.12 and 0.18 mm, were arbitrarily chosen and applied. The specimen details are given in Table 2.

Rectangular specimens of size 50 × 300 mm were used in the experiments to determine the residual stresses due to the indentation process. The specimen material and preparation procedures were identical to that of fatigue test specimens as described in Table 2. A crack in the form of a saw cut of length 12 mm in the direction transverse to the long axis of the plate specimen was introduced at one edge of the plate. The relative displacement between points c and c', separated by a distance of 25 mm (see Fig. 4) was measured using an extensometer. The crack was extended simultaneously in a stepwise manner with increments of 1 mm until the

Table 2
Classification of the fatigue test specimens

Specimen	Width of circular ring, w (mm)	Indentation load, p (KN)	Indented depth, b (mm)	Distance, h (mm)
1	0.5	20	0.06 ± 0.01	3
2		23	0.12 ± 0.01	
3		24	0.18 ± 0.01	
4	0.7	24	0.06 ± 0.01	
5		27	0.12 ± 0.01	
6		29	0.18 ± 0.01	
7	1.0	30	0.06 ± 0.01	
8		34	0.12 ± 0.01	
9		36	0.18 ± 0.01	
10	0.5	23	0.12 ± 0.01	1
11				3
12				5
13	0.7	27		1
14				3
15				5
16	1.0	34		1
17				3
18				5

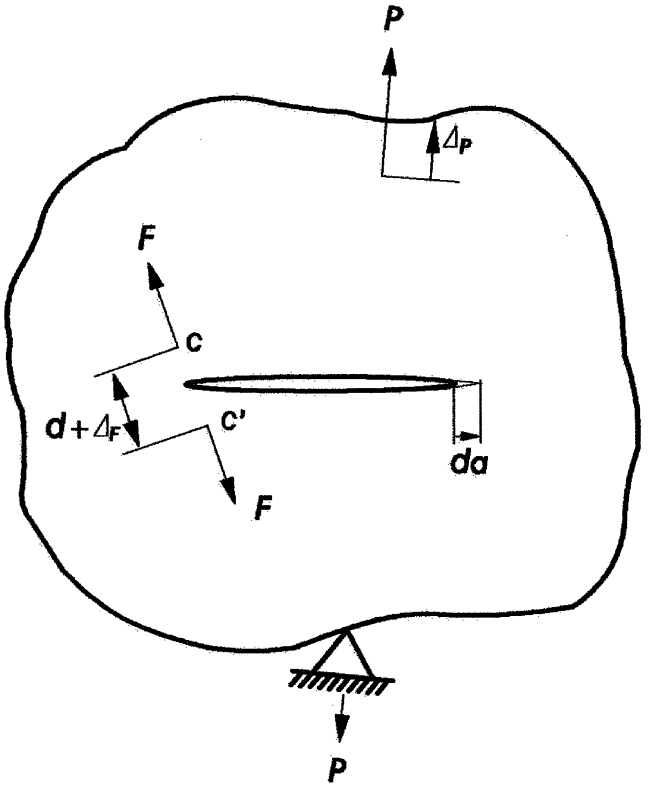

Fig. 3. A body loaded by forces, P and virtual forces, F.

crack length reached 22 mm. The residual stress distribution around the crack was then computed from the measured displacements. The theory of residual stress measurement is given in the next section.

The fatigue crack growth testing was carried out in a 100 kN capacity Instron electro-hydraulic material test system with stress ratio $R = 0.1$. The specimens were fatigue tested with constant amplitude sinusoidal loading at a rate of 12 Hz in a laboratory atmosphere. One face of the specimens was polished to a good surface finish around the center region so as to facilitate ease of subsequent crack growth measurements. A traveling microscope was used to measure the crack lengths while the specimens were mounted in the machine. Three specimens for each type were tested and one of test records was chosen.

3. Evaluation of residual stresses

3.1. Relative displacements of crack surfaces

In order to evaluate the residual stresses around a crack from ring indentation, the fracture mechanics approach proposed by Kang et al. [9] was employed in the present study. Consider a body loaded by forces, P, which in addition has virtual forces, F, applied, as shown in Fig. 3. Then letting the virtual forces to approach zero, the displacement, Δ_F between points c and c' can be derived as [10]

$$\Delta_F = \Delta_{F\ \text{no crack}} + \frac{2}{E'}\int_0^a \left[K_{IP}\frac{\partial K_{IF}}{\partial F} + K_{IP}\frac{\partial K_{IIF}}{\partial F}\right] \mathrm{d}a \quad (1)$$

where K_{IP} and K_{IIP} are the stress intensity factors due to P for mode I and II, respectively, and K_{IF} and K_{IIF} are those due to virtual forces, F. E' is a parameter with $E' = E$ for plane stress and $E' = E/(1-\nu^2)$ for plane strain and E and ν represent Young's modulus and Poisson's ratio, respectively.

The stress intensity factor for the crack in a residual stress field can be written as [11]

$$K_I^r = \int_A m(x,a)\sigma_y^r(x)\ \mathrm{d}x \quad (2)$$

where $m(x,a)$ is the weight function for a given geometry, A is crack face length, and σ_y^r is the normal component of residual stress at the prospective crack calculated for the uncracked body. Substituting K_I^r of Eq. (1) into K_{IP} of Eq. (1) and allowing K_{IIP} and $\Delta_{F\ \text{no crack}}$ to be zero, the displacement, Δ_F, can be simplified to

$$\Delta_F = \frac{2}{E'}\int_0^a \left[K_I^r\frac{\partial K_{IF}}{\partial F}\right] \mathrm{d}a \quad (3)$$

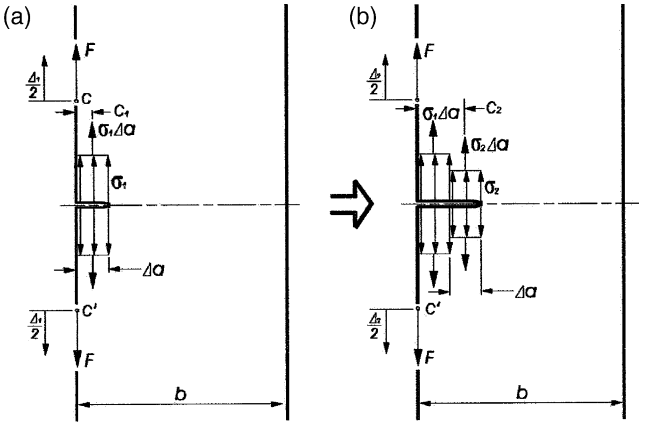

Fig. 4. Single edge cracks in a finite width plate. (a) The residual stress σ_1 released by introducing a crack length Δa. (b) The residual stress σ_2 released by increasing a crack length Δa.

3.2. Determination of residual stress

When there are residual stresses along the line of a single edge crack, introduction of a crack emanating from the edge of the plate will release the residual stresses. Assuming that the residual stress, σ_1, is constant in the interval, Δa, we can replace it by a concentrated force, $\sigma_1\Delta a$ applied at the point of distance, c_1 as shown in Fig. 4. The stress intensity factor due to $\sigma_1\Delta a$ is then derived from Eq. (2) and is given as

$$K_I^r = 2\int_0^{a_1} \sigma_1 \Delta a \delta(x-c_1) m(x,a_1)\ \mathrm{d}x \quad (4)$$

$$= 2\sigma_1 \Delta a m(c_1,a_1)$$

where $\delta(x-c_1)$ is Dirac's delta function, $c_1 = \Delta a/2$, a_1 is the length of the present crack ($a_1 = \Delta a$ in this case) and $m(x,a)$ is the weight function for single edge crack emanating from an edge in a finite plate given by Wu and Carlsson [12]

$$m(x, a_1) = \frac{1}{\sqrt{2\pi a_1}} \sum_{i=1}^{3} \beta_i(a) \left(1-\frac{x}{a}\right)^{i-3/2} \quad (5)$$

$$\beta_1(a) = 2.0$$

$$\beta_2(a) = \left[4af'_r(a) + 2f_r(a) + \frac{3}{2}F_2(a)\right] \Big/ f_r(a)$$

$$\beta_3(a) = \left\{aF'_2(a) + \frac{1}{2}[5F_3(a)-F_2(a)]\right\} \Big/ f_r(a)$$

$$\beta_4(a) = \left\{aF'_3(a) + \frac{1}{2}[7F_4(a)-3F_3(a)]\right\} \Big/ f_r(a)$$

$$\beta_5(a) = \left[aF'_4(a) - \frac{5}{2}F_4(a)\right] \Big/ f_r(a)$$

$$F_1(a) = 4f_r(a)$$

$$F_2(a) = \frac{1}{12\sqrt{2}}\left[315\pi\psi(a) - 105V_r(a) - 208\sqrt{2}f_r(a)\right]$$

$$F_3(a) = \frac{1}{30\sqrt{2}}\left[-1260\pi\psi(a) + 525V_r(a) + 616\sqrt{2}f_r(a)\right]$$

$$F_4(a) = \sqrt{2}V_r(a) - [F_1(a) + F_2(a) + F_3(a)]$$

$$\psi(a) = \frac{1}{a^2}\int_0^a s[f_r(s)]^2\ \mathrm{d}s$$

where $f_r(a)$ and $V_r(a)$ are defined as

$$f_r(a) = K_r/\sigma\sqrt{\pi a W}$$

$$V_r(a) = E' u_r(a,0)/\sigma a$$

The stress intensity factor due to virtual forces, K_{IF} shown in Fig. 4 is determined similarly from Eq. (2) and is given by

$$K_{IF} = 2\int_0^a m(x,a)\sigma_y^F(x)\ \mathrm{d}x \quad (6)$$

where $\sigma_y^F(x)$ is the normal stress distributed along the x-axis of the uncracked strip due to a pair of forces, F, and which is determined by using a finite element analysis.

$$\sigma_y^F(x) = F\left[A_0 + A_1 x + A_2 x^2 + \ldots + A_8 x^8\right] \quad (7)$$

Substituting Eqs. (4) and (6) into Eq. (3), the relative displacement, Δ_1, between c and c' due to the introduction of a crack, whose length is Δa can be obtained as

$$\frac{1}{2}\Delta_1 = \frac{4}{E'}\sigma_1 \Delta a \int_{c_1}^{a_1} m(c_1, a)h(x, a)\ \mathrm{d}a \quad (8)$$

$$h(x,a) = 2\int_0^a m(x,a)\frac{\partial \sigma_y^F(x)}{\partial F}\mathrm{d}x$$

On further extending the crack length from Δa to 2 Δa as shown in Fig. 4, the relative displacement, Δ_2, can be expressed as

$$\frac{1}{2}\Delta_2 = \frac{4}{E'}\sigma_1 \Delta a \int_{c_1}^{a_2} m(c_1,a)h(x,a)\ \mathrm{d}a \quad (9)$$

$$+ \frac{4}{E'}\sigma_2 \Delta a \int_{c_2}^{a_2} m(c_2,a)h(x,a)\ \mathrm{d}a$$

Similar equations for the relative displacements, Δ_3, Δ_4, …, Δ_n can be obtained by extending the crack further. The residual stresses are thus determined using these equations.

4. Results and discussion

4.1. Residual stress

Fig. 5 shows the distribution of residual stresses introduced into the material surrounding the crack by the process of ring indentation. In order to investigate the effects of indentation depth on the distribution of

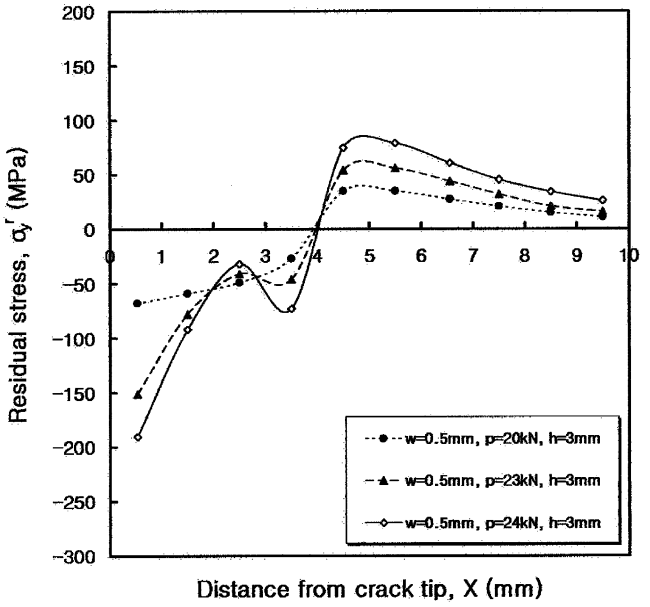

Fig. 5. Effect of indentation load on the distribution of residual hoop stresses, showing that compressive residual stress is increased more for increasing indentation load.

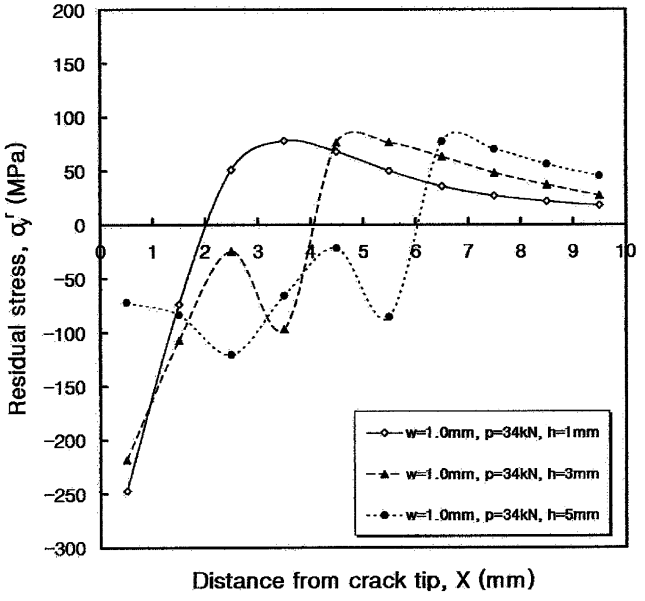

Fig. 6. Effect of indented position on the distribution of residual hoop stresses, showing that compressive residual stress is increased more for closer indentation.

residual stresses, the indentation was located at $h = 3$ mm by using the ring punch with a thickness of 0.5 mm. The solid line in the figure is obtained with the indentation depth of 0.18 mm, the dashed and dotted lines are obtained with the indentation depth of 0.12 and 0.06, respectively. It can be observed that complex residual hoop stress fields are introduced around the crack by ring indentation. The stresses are due to the local deformation of material adjacent to the punch. It can be seen that the process provided a significant increase in compressive residual stresses in the region immediately adjacent to the surface of the crack. The compressive residual stresses around the crack increase as the relative indentation depth increases. It is closely related to the indentation load.

The effects of punch location on the distribution of residual stresses around the crack are shown in Fig. 6. The indentation was located at three different distances, $h = 1$, 3 and 5 mm. Specimens were indented by using the ring punch with a thickness of 1 mm. The indentation depth was 0.12 mm. It can be observed that the compressive residual stresses around the crack tip increase as the indentation is located in a region immediately adjacent to the surface of the crack. The indentation distance $h = 1$ mm gives the biggest increase of compressive residual stress at the crack tip. The figure shows that although the induced compressive stress at the crack tip is somewhat less when the punch is farther away, the effect actually extends over a greater distance and actually varies considerably more than one might expected.

4.2. Fatigue crack growth

All specimens listed in Table 2 were fatigue tested to failure. This allowed a comparison of fatigue crack growth behavior of ring-indented specimens and non-indented specimen. Fig. 7 depicts the crack growth comparison of ring-indented cracks. In order to investigate the effects of indentation load on crack growth curves, the indentation was located at $h = 3$ mm by using three different types of ring punch as noted previously. The

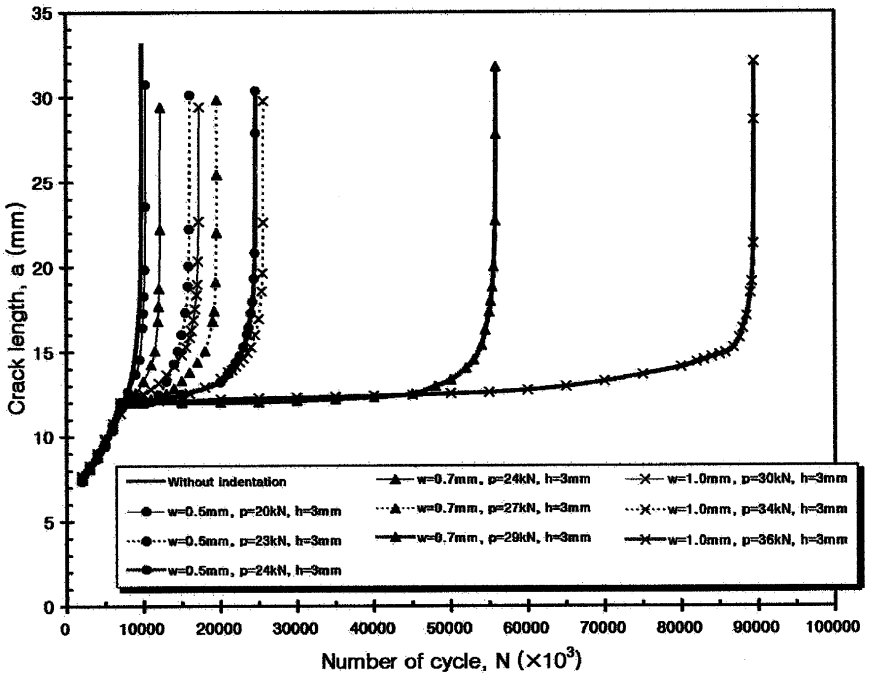

Fig. 7. Effect of indentation load on crack growth curves, showing that crack growth is retarded more for increasing indentation load.

results are compared with that for the non-indented specimen, which is represented by a solid line. It can be observed that the lowest indentation load (20 kN) with 0.5 mm thick ring punch creates little difference in the fatigue data over non-indentation, but when the indentation load is increased, its effect is seen in crack growth. Similar results were obtained from specimens indented by other ring punches. Fig. 7 shows that increased indentation load results in increased fatigue life, for all three punches used. For the case of specimens indented to the same depth, a ring having a larger width is more beneficial for crack retardation. It is also closely related to the indentation load, which increases with the width of the ring punch. Consequently it can be concluded that the retardation of crack is clearly related to the indentation load. This phenomenon has a relation to the distribution of compressive residual stresses around the crack as shown in Figs. 5 and 6, and crack growth is further retarded with increasing compressive residual stresses.

The effects of indented position on crack growth curves are presented in Fig. 8. The indentation process was performed using three different types of ring punches at distances h = 1, 3, and 5 mm, respectively. The indented depth for all specimens was 0.12 mm. It can be observed that the crack retardation increases as the indentation is closer to crack tip for a given ring punch. The indentation process is therefore very beneficial in terms of total fatigue life. The number of cycles to failure for specimens BP1(27) and CPI(34) increased by about 2.3 and 2.8 times, respectively, compared to specimens BP5(27) and CP5(34).

Fig. 9 shows the fatigue crack growth rate as a function of crack length for three specimens indented using the ring punch with a thickness of 1.0 mm. The specimens were indented at a distance of h = 3 mm. The retardation of growth rate was clearly observed when the crack had grown into the indentation area. A possible reason for this phenomenon in crack growth rate is the distribution of compressive residual stresses inside the

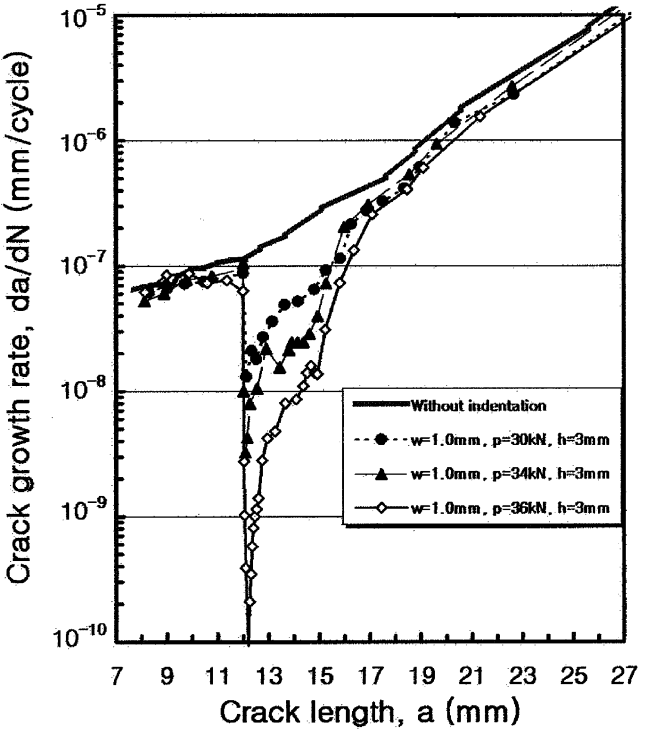

Fig. 9. Effect of indentation load on fatigue crack growth rate, showing that da/dn is retarded more for increasing indentation load.

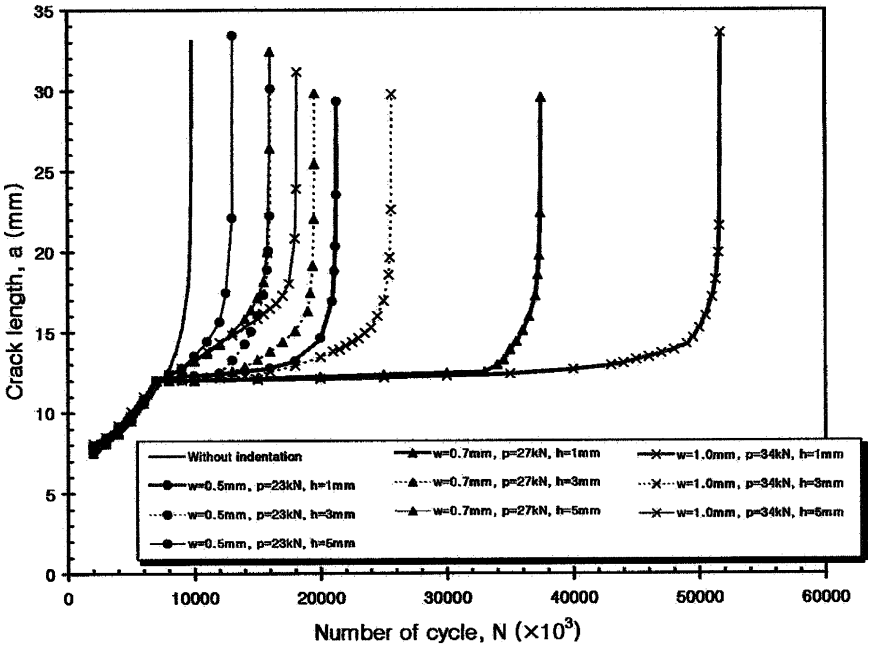

Fig. 8. Effect of indented position on crack growth curves, showing that crack growth is retarded more for closer indentation.

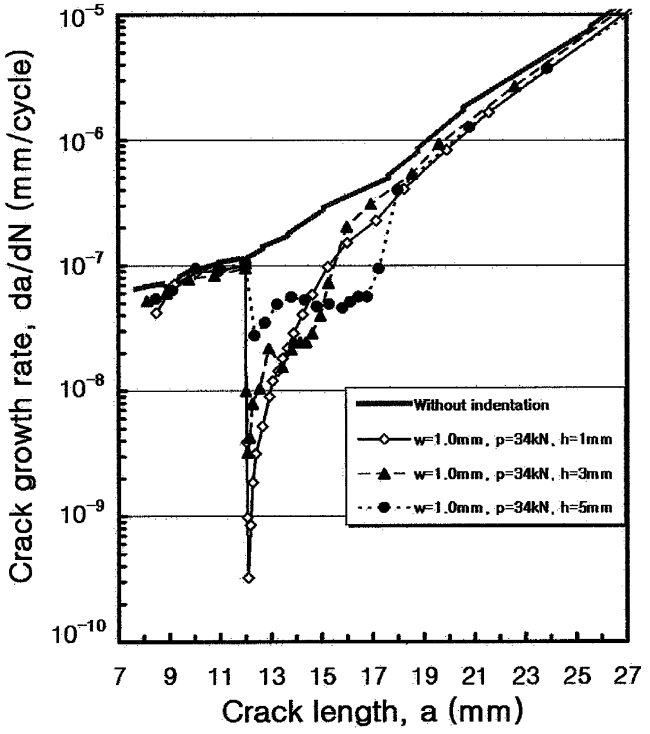

Fig. 10. Effect of indented position on fatigue crack growth rate, showing that d*a*/d*n* is retarded more for closer indentation, but retardation is over a smaller distances.

indentation area. It can be seen that the retardation effect increases as the indentation load increases. On the other hand, when the crack passes through the indentation area the growth rate increases rapidly and then becomes equal to that of the non-indented specimen. This sudden increase of growth rate may be explained in terms of the tensile residual stresses outside the indentation area, and the slight variation of specimen thickness due to indentation and the stress concentration at the indentation groove.

The fatigue crack growth rate vs. crack length for specimens with indentation depth of 0.12 mm is shown in Fig. 10. The indentation process was performed using three different types of ring punch at distances of h = 1, 3, and 5 mm. It is shown that the indentation process is very beneficial for crack retardation when the indentation is located in closer range to the crack tip.

5. Conclusions

The results show that for the testing conditions considered, the indentation around a crack by ring punch caused negligible retardation. Experimental procedures were given to define residual stress distributions surrounding the crack tip. The induced compressive stress at the crack tip is somewhat less when the punch is far away, the effect actually extends over a greater distance and actually varies considerably more than one might expect. Increased indentation load results in increased fatigue life. Fatigue crack growth is retarded more for closer indentation, but retardation is over a smaller distance.

References

[1] Chen D-H, Nisitani H. Eng Fract Mech 1991;39:287.
[2] Song S-H, Choi J-H, Kim K-S, Choi B-K. Trans KSME 1998;22(10):1806 [in Korean].
[3] Hertzberg RW. Deformation and fracture mechanics of engineering materials. John Wiley & Sons; 1976 p. 237.
[4] Song S-H, Choi J-H. Trans KSME 1998;22(10):1798 [in Korean].
[5] Goto M, Nisitani H, Miyagawa H, Imada K. Trans JSME 1990;56(526):1348 [in Japanese].
[6] Sehgal MM, Kobayashi S. ASME J Eng Industry 1972;November:1035.
[7] Lee KY, Kang JM. Trans KSME 1984;8:313 [in Korean].
[8] Lim W-K, Yoo J-S, Choi S-Y. Eng Fract Mech 1998;59(5):643.
[9] Kang KJ, Song JH, Earmme YY. J Strain Anal Eng Des 1984;45:23.
[10] Tada H, Paris P, Irwin G. The stress analysis handbook. Del Res Co; 1985 p. B1.
[11] Parker AP. ASTM STP 776, 1982. p. 13.
[12] Wu XR, Carlsson AJ. Weight functions and stress intensity factor solutions. NY: Pergamon; 1991. p. 104.